
# GEE-based Analysis of LULC Changes Across Five Decades Over Part of Northern India

Pranjal Pandey

Environmental Science and Engineering Department, Indian Institute of Technology Bombay, Mumbai, India.

*(Received: 21.10.2025; Accepted: 01.11.2025)*
**Web link:** https://ijths.com/volume-1-issue-2-october-december/

***Abstract***

*In this paper, we examine the change in the land use pattern in and around three major seasonal rivers (Ghaggar, Markanda, and Tangri) and two minor streams marked as Stream A and Stream B of northern Haryana and Punjab region (India) due to urbanisation and agricultural practices. Landsat data covering a period of 50 years, which includes Landsat 1 MSS (1973) at 60m resolution and Landsat 8 OLI/TIRS (2023) at 30m resolution, are used. Google Earth Engine-based Land Use Land Cover modeling is used for all analysis. A comparison of classified images at a difference of 50 years suggests major part of the flood plains of all three main rivers is occupied by urbanisation as well as converted to agricultural land. The study shows that the builtup area has increased by 552.43 sq. kms. and the water area in terms of ponds, etc., has increased by 7.31 sq. kms. whereas a reduction of 93.31 sq. kms. in the vegetation area was observed. Further, the bare open land area is found to be reduced by 466.44 sq. kms. Thus, suggesting encroachment in the river floodplain and bare open land due to excessive urbanisation and agricultural practices.*

***Keywords:*** *Land use land cover (LULC); Google Earth Engine (GEE); Landsat; Geographical information system (GIS); Transition analysis*

## INTRODUCTION

Urbanisation is causing a significant impact on the natural environment, with over half of the world's population presently living in cities and predicted to reach 66% by 2050 (WHO, 2025). This significant increase in human population led to an increase in anthropogenic activities such as industrialisation, urbanisation, agricultural expansion, etc., which have adverse impacts on the environment (Chen *et al.*, 2014). Land Use Land Cover (LULC) changes are critical indicators of environmental dynamics influenced by both natural and anthropogenic activities (Nugroho *et al.*, 2018). The trend has shown that with increasing population over time, the land near the river basin has been occupied by humans for different purposes. This urbanisation-induced drainage system degradation causes severe flooding and, occasionally, the loss of life and property in the floodplain (Nabegu, 2014; Ibitoye *et al.*, 2020). Urbanisation is regarded as an irreversible phenomenon that modifies the earth's surface (Chin, 2006), suggesting that monitoring and management of urban growth remains a critical focus. Monitoring and evaluating the performance of urban drainage systems is also essential, as they play a vital role in mitigating urban flooding. The use of GIS-based techniques (Lui and Coomes, 2015) and geospatial methodologies, including Remote Sensing (RS), the data provides valuable information for observing, detecting, and analyzing the impacts of long-term alterations in land use land cover patterns including natural drainage systems due to urbanization (Miller and Hess, 2017). The ability to show the channel layout over time as a result of anthropogenic activities or natural phenomena like floods was made possible by a time series of satellite images (Sarker, 2022). Satellite imagery that is freely accessible and offers consistent global coverage serves as an essential tool for land use land cover monitoring (Yousefi *et al.*, 2013). Advancements in spatial resolution over time have significantly enhanced their utility, especially for the observation of river flood plains including those around smaller rivers. Several studies have utilized satellite images to evaluate and monitor changes in river morphology (Zheng *et al.*, 2018; Nones, 2021; Kausarian *et al.*, 2023; Moldakhanova *et al.*, 2023). Additionally, studies have

provided a relationship between urbanization and the reduction in river floodplains, offering useful resources for local river management and conservation (Zope *et al.*, 2016; Xu *et al.*, 2018; Han *et al.*, 2020). Historical knowledge of LULC and evaluation of its change, as well as triggering variables, are critical for understanding the current phenomenon and developing suitable land use planning for the conservation of environmental system functioning at all scales (Yermekbayev *et al.*, 2023; Yussupov and Suleimenova 2023). These changes have a negative impact on the environment and human life by influencing land patterns, hydrological networks, water quality, and budget (Aduah *et al.*, 2018; Inalpulat and Genc, 2021; Pranoto *et al.*, 2023).

Studies have analysed the quantitative and qualitative changes in land use and land cover (LULC) patterns and their drivers using various approaches and techniques, including an expert system classification approach for detailed mapping of urban LULC changes (Napieralski and Carvallhaes, 2016; Wentz *et al.*, 2023). An indices-based index to map builtup expansion in cities and its relationship with population growth and distribution also suggests the primary driving forces behind LULC changes are population growth and urbanisation (Msofe *et al.*, 2019; Shahfahad *et al.*, 2021).

Given the above-cited studies, the presented work was planned to study the change in LULC over the last 5 decades (1973–2023) and its influence on the major season rivers/floodplains in part of Haryana and Punjab states in Northern India.

## MATERIALS AND METHODS

### Study Area

The study area encompasses portions of Haryana and Punjab states (Northern India), as shown in Fig. 1, both situated within a tropical monsoon climate characterised by hot summers, a monsoon season, and cool winters. Rainfall exhibits spatial variability across the region. Five perennial streams traverse the study area, three of which are identified as the Ghaggar, Markanda, and Tangri. The Tangri and Markanda flow primarily within the Ambala and Kurukshetra districts of Haryana, while Stream A and Stream B are situated within the Mohali district of Punjab. The Ghaggar River flows through both states, covering the Patiala district of Punjab and the Ambala district of Haryana with a more significant presence in Punjab.

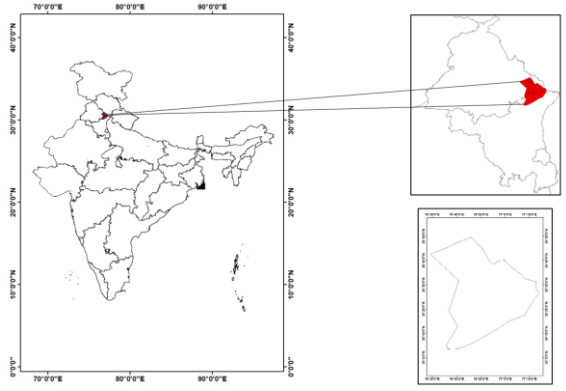

**Fig. 1:** Study area.

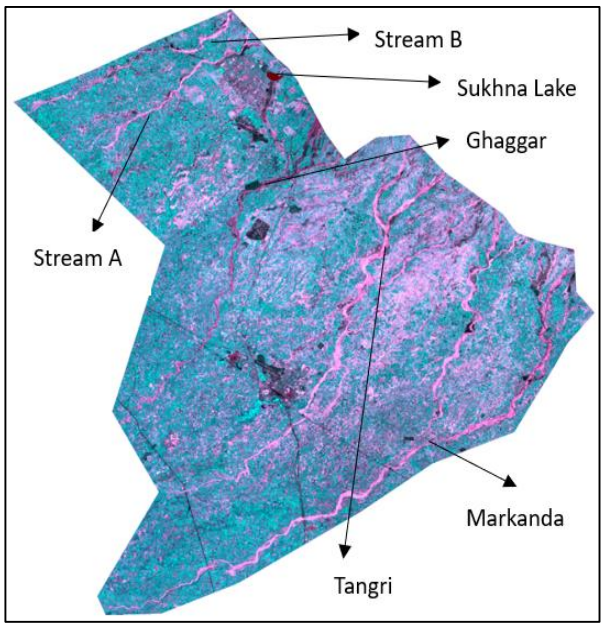


**(a)**

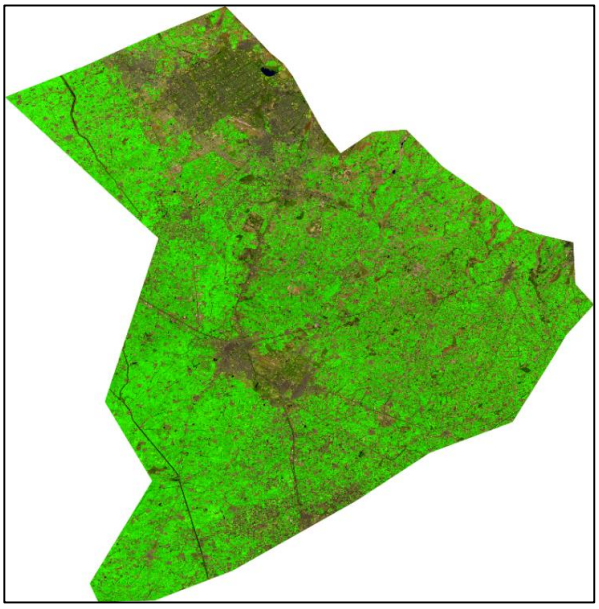

**(b)**

**Fig. 2:** Landsat images: **(a)** Landsat 1 MSS 1973 (60 m resolution); **(b)** Landsat 8 OLI/TIRS 2023 (30 m resolution).

### Data Collection

Fig. 2 provides Landsat images used in this work and covers the study area. The first image, Fig. 2a, was captured on 03rd March 1973 using Landsat 1 at 60m resolution. This image comprises of 4 bands i.e: B4(Green), B5(Red), B6(Near Infrared 1) and B7(Near Infrared 2). Fig. 2b represents the Landsat 8 image of the study area acquired on 25th February 2023 at a resolution of 30m. The image used in the present work comprises seven bands, namely SR_B1(Ultra Blue), SR_B2(Blue), SR_B3(Green), SR_B4(Red), SR_B5(Near Infrared), SR_B6(Shortwave Infrared 1) and SR_B7(Shortwave Infrared 2), in comparison of four bands

of the Landsat 1 image.

### Data Analysis

The analysis of both images is carried out using Google Earth Engine (GEE). To study the change in land use patterns over 5 decades covering the study area, supervised classification was used to classify both images into four major land cover classes (i.e. Water bodies, Vegetation, Builtup area, and Bare Open Land). When it comes to mapping the land cover of vast regions, GEE, a cloud-based computing platform, can resolve the most important issues. Without downloading the data to their local computer, users can use an online Integrated Development Environment (IDE) code editor to examine all of the remotely sensed images that are available. This makes it simple for users to access, choose, and process vast amounts of data for a wide range of research topics (Gorelick *et al.*, 2017; Phan *et al.*, 2022). A significant factor behind GEE's increasing popularity, in addition to its quick processing speed, is the availability of multiple packages with numerous algorithms that make it easier for both experts and non-experts to access remote sensing tools. To reduce the ambiguity in classification over the 50-year period over the study area, only the 'vegetation" land cover class is considered in place of both sparse vegetation and crops in classifying both images. The process of supervised classification involves creating quality training data by manually marking representative regions for each class in both Landsat images (Table 1).

**Table 1.** Number of samples from 1973 and 2023 data.

| Parameter | Number of samples | |
|---|---|---|
| | 1973 | 2023 |
| Water | 81 | 156 |
| Vegetation | 299 | 284 |
| Builtup | 33 | 303 |
| Bare open land | 195 | 225 |
| Total | 608 | 968 |

Prior to performing supervised classification on the Landsat 1 dataset, a resampling process was used so as to convert the original 60-meter pixels to a 30-meter pixel size. This was done keeping in view of the 30 m resolution of the Landsat 8 image. As the aim of this study was to compare the area under each class, the same spatial resolution was used with both datasets. The NDVI and NDWI indices (Fig. 3) were also used as input for the classification of data from 1973 and 2023 (Table 2). Additionally, the NDBI index (Fig. 3e) was included alongside these two indices in the 2023 data. The availability of only four bands makes it difficult to drive these

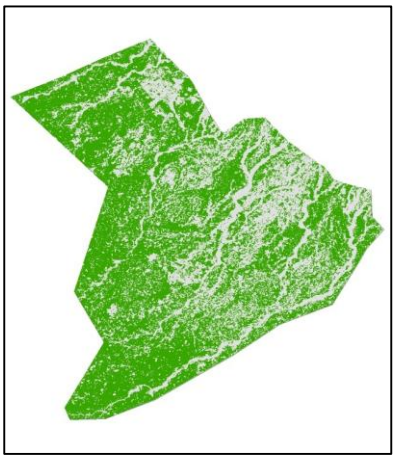

**(a)** NDVI layer: 1973

**(b)** NDVI layer: 2023

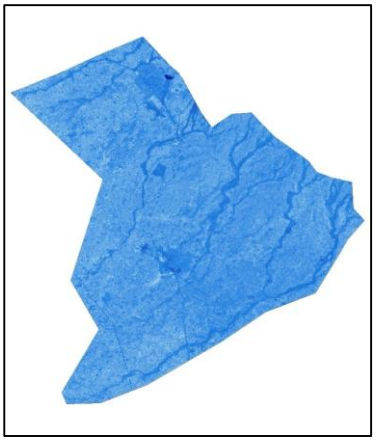

**(c)** NDWI layer: 1973

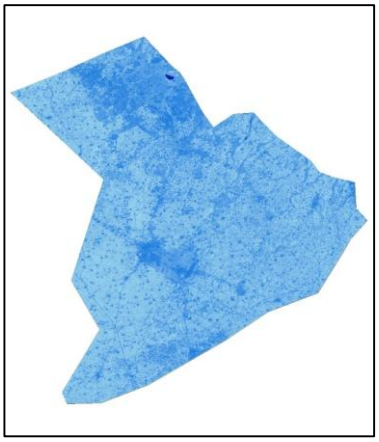

**(d)** NDWI layer: 2023

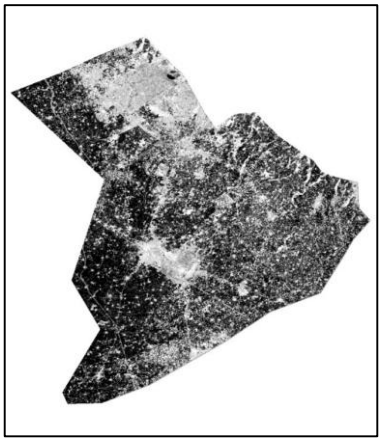

**(e)** NDBI layer: 2023

**Fig. 3:** NDVI and NDWI layers of 1973 and 2023, and NDBI layer of 2023.

**Table 2.** Spectral indices used in the study

| Index | Equation |
|---|---|
| Normalized Difference Water Index ($NDWI$) | $\frac{Green - NIR}{Green + NIR}$ |
| Normalized Difference Builtup Index ($NDBI$) | $\frac{SWIR - NIR}{SWIR + NIR}$ |
| Normalized Difference Vegetation Index ($NDVI$) | $\frac{NIR - Red}{NIR + Red}$ |

indices with the 1973 dataset.

Out of the total samples, 80% were used for training; whereas, the rest for testing the performance of the used classifier. These labeled samples are then used to extract spectral information from the input imagery. A Random Forest (RF) classifier, which is found to perform well in other studies is used in this study. The trained model is then applied to the entire image to classify all pixels based on their spectral properties. The results are evaluated using a confusion matrix to assess accuracy, with test data.

Being of 60 m pixel size, obtaining sufficient quality training/testing pixels was a problem with 1973 data hence a limited number of pixels are used in classifying this dataset. The availability of a limited builtup area in the study area in 1973 is a major reason for the small number of builtup pixels (Table 1).

The Random Forest (RF) classifier implemented in GEE is a supervised classifier that works by creating an ensemble of decision trees to classify pixels in satellite imagery. A random subset of the training data is used to train each decision tree in the forest using a set of input features to ensure diversity and reduce overfitting. During classification, to give each pixel a class, the algorithm aggregates the predictions of every tree using majority voting. In GEE, the process begins by preparing training data (labelled samples) and extracting spectral and other feature information from the imagery.

The RF algorithm is then trained on this dataset, defining two user-defined parameters, i.e. the number of trees and the maximum number of features used to generate a tree. In this study, the optimum number of trees for maximum accuracy has been obtained by performing hyperparameter tuning. The optimum number of trees was 200 to achieve maximum accuracy for the 1973 dataset, and is 10 for the 2023 dataset. Further, the number of features used to generate trees with both datasets was the default value in GEE, that is, sqrt (total number of features). With the 1973 and 2023 datasets, the total number of features used for analysis was 6 and 10, respectively. Once trained, the model is applied to the entire image to produce a classified map. RF is popular in GEE due to its robustness, high accuracy, and ability to handle large datasets with complex, non-linear relationships between input features. Further, transition analysis has been performed to understand and quantify the individual conversion of each land cover class into another.

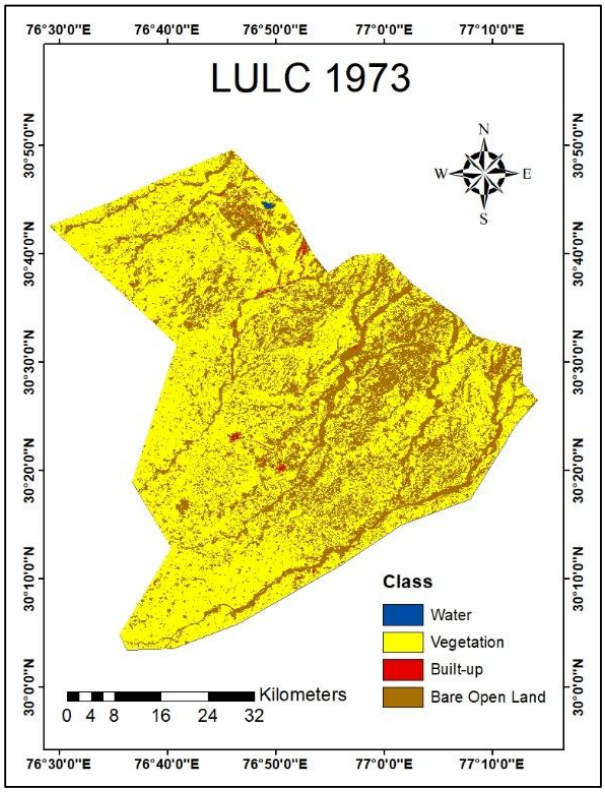


**(a):** 1973

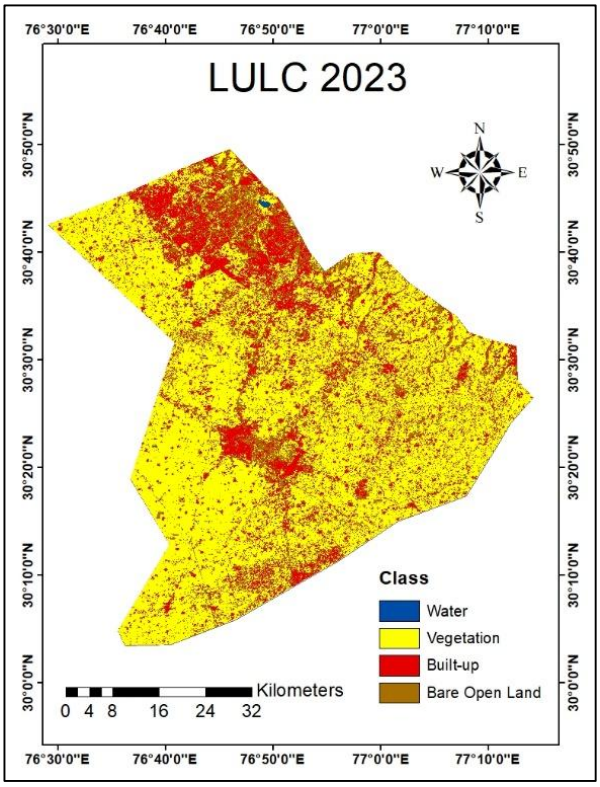


**(b):** 2023

**Fig.4:** LULC of study area.

## RESULTS

After performing the supervised classification on both datasets of 1973 and 2023 (Fig. 4), the Land cover and usage data obtained are shown in Tables 3 and 4. In Table 3, a small error in total area calculation was observed between the 1973 and 2023 datasets, which is possibly due to resampling of 60m pixel to 30m pixel. Classification accuracy is provided

**Table 3.** Land use land cover of study area.

| Parameter | Area : 1973 | | Area : 2023 | |
|---|---|---|---|---|
| | sq. kms. | % | sq. kms. | % |
| Water | 1.42 | 0.045 | 8.73 | 0.278 |
| Vegetation | 2,103.42 | 66.864 | 2,010.11 | 63.898 |
| Builtup | 15.62 | 0.497 | 568.05 | 18.057 |
| Bare open land | 1,025.34 | 32.594 | 558.90 | 17.767 |
| Total | 3,145.80 | 100.000 | 3,145.79 | 100.000 |

**Table 4.** Quantitative changes in LULC in Study Area.

| Class | Area increase/decrease 1973 to 2023 | |
|---|---|---|
| | sq. kms. | % |
| Water | +7.31 | +0.233 |
| Vegetation | -93.31 | -2.966 |
| Builtup | +552.43 | +17.560 |
| Bare open land | -466.44 | -14.827 |

in Tables 5 and 6.

Tables 3 and 4 present the quantitative changes in land use and land cover in a study area between 1973 and 2023. A comparison of results from these tables suggests a significant decrease in bare open land cover (+14.827%) amounting to a loss of 466.44 sq. kms. in the study area during the study period. The decrease in bare open land cover is likely

**Table 5.** Accuracy assessment

| Class | 1973 | | 2023 | |
|---|---|---|---|---|
| | Producer's accuracy | User's accuracy | Producer's accuracy | User's accuracy |
| Water | 100.00 | 100.00 | 100.00 | 100.00 |
| Vegetation | 98.38 | 100.00 | 100.00 | 100.00 |
| Builtup | 57.14 | 57.14 | 98.46 | 100.00 |
| Bare open land | 91.42 | 88.88 | 100.00 | 98.07 |

**Table 6.** Overall classification accuracy.

| Class | 1973 | 2023 |
|---|---|---|
| Overall Classification Accuracy | 94.30% | 99.50% |
| Kappa Statistics | 0.9110 | 0.9933 |

attributed to factors such as deforestation, urbanization, and infrastructure development. Conversely, builtup areas have seen a substantial increase (+17.560%), gaining about 522.43 sq. kms. The substantial increase in builtup areas is indicative of rapid urbanization and population growth. This expansion often leads to the conversion of agricultural land, forests, and natural habitats into urban settlements, infrastructure, and industrial areas. Water bodies have also witnessed a modest increase (+0.233%), gaining 7.31 sq. kms., Vegetation, on the other hand, has experienced a decrease (-2.966%), losing 93.31 sq. kms. The decrease in vegetation could be due to various reasons, including rapid urbanisation, agricultural

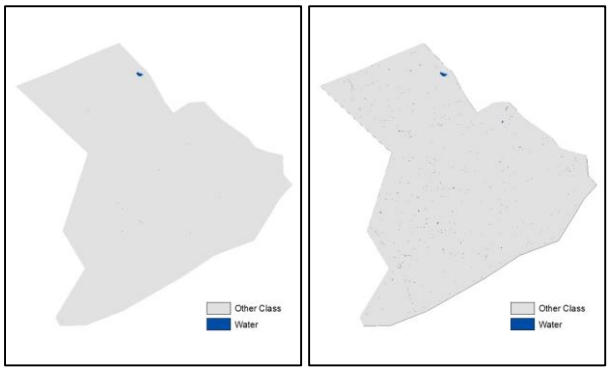


1973 2023

**(a)** Water: 1973-2023

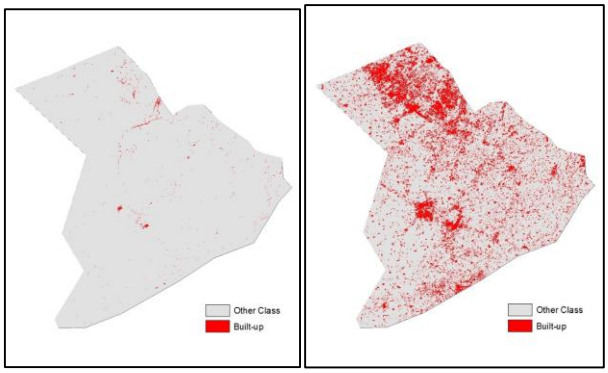


1973 2023

**(b)** Builtup: 1973-2023

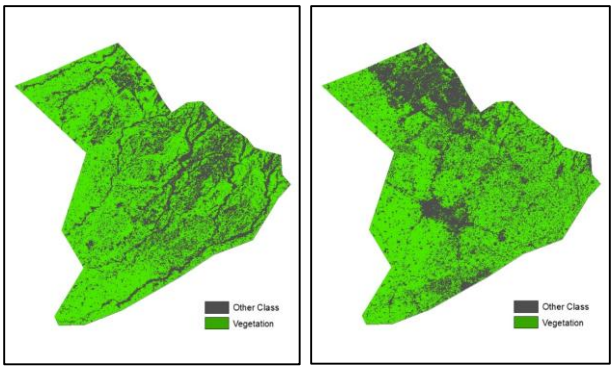


1973 2023

**(c)** Vegetation: 1973-2023

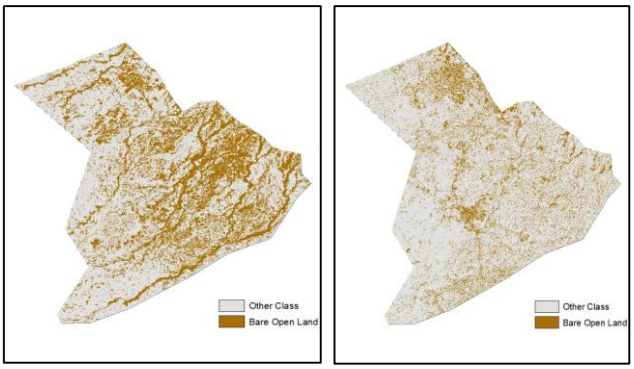


1973 2023

**(d)** Baren open land: 1973-2023

**Fig. 5:** Variation of classes from 1973-2023.

expansion, land reclamation projects, and others.

A comparison of Figs. 5a and 5b indicate that increased urbanisation and agricultural activities have occupied a large part of the flood plains of seasonal rivers, a reason for the non-visibility of river channels in Fig. 3b. This encroachment of the floodplain is becoming a major reason for floods in the nearby areas of these seasonal rivers.

Further, four different images of each class for both 1973 and 2023 were obtained by performing single-class detection analysis, where a value '1' has been assigned to one class and '0' to other classes. From Fig. 5a, it can be seen that from 1973 to 2023 the water area has increased due to the creation of artificial water bodies such as canals, ponds, ditches, etc., used for agriculture and other purposes. Further, Fig. 5b indicates an increase in builtup area; whereas, Figs. 5c and 5d suggest a decline in the area under vegetation and bare open land from 1973 to 2023. This decline in bare land may be attributed to an increase in area under agricultural and builtup area categories.

Fig. 6 illustrates the transition of land cover class from 1973 to 2023. Each category displays the area that transitioned from its 1973 state to a different class in 2023. Fig. 6 also reveals that the land area belonging to the streams Ghaggar, Markanda, Tangri, Stream A, and Stream B up to 1973 has undergone a significant transition to different land cover types by 2023.

Table 7 presents a comprehensive overview of land use and land cover (LULC) changes within a specific region over a 50-year period. It provides the transitions between four primary land cover types: Water, Vegetation, Builtup areas, and Bare Open Land. The data provides quantitative insights into the extent of land cover transformations. Each row in the table represents a specific transition pathway. Tables 5 and 6 provide the user's and producer's accuracy as well as overall classification accuracy with both datasets.

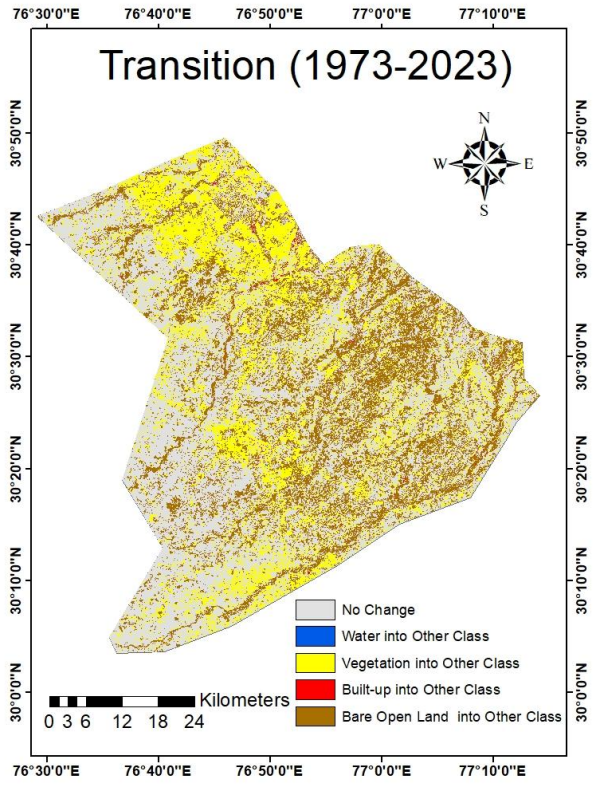


**Fig. 6:** Transition: 1973-2023.

**Table 7.** Overall classification accuracy.

| Transition | Area (sq. kms.) |
|---|---|
| Water1973 into Water2023 | 1.20 |
| Water1973 into Vegetation2023 | 0.07 |
| Water1973 into Builtup2023 | 0.06 |
| Water1973 into BareOpenLand2023 | 0.10 |
| Vegetation1973 into Water2023 | 3.65 |
| Vegetation1973 into Vegetation2023 | 1,433.23 |
| Vegetation1973 into Builtup2023 | 341.96 |
| Vegetation1973 into BareOpenLand2023 | 324.58 |
| Builtup1973 into Water2023 | 0.15 |
| Builtup1973 into Vegetation2023 | 4.23 |
| Builtup1973 into Builtup2023 | 6.01 |
| Builtup1973 into BareOpenLand2023 | 5.23 |
| BareOpenLand1973 into Water2023 | 3.73 |
| BareOpenLand1973 into Vegetation2023 | 572.58 |
| BareOpenLand1973 into Builtup2023 | 220.02 |
| BareOpenLand1973 into BareOpenLand2023 | 229.00 |

## DISCUSSION

Urbanisation significantly exacerbates flooding by altering natural hydrological processes. Rainwater penetration into the soil is decreased when cities grow because permeable landscapes are replaced with impervious surfaces like parking lots, buildings, and roadways. This leads to increased surface runoff during rainfall events, overwhelming drainage systems and causing localised flooding. In the study area, results from Table 4 indicate that in both the two classes that show significant changes, i.e. vegetation and bare open land, a major land area has been converted into the builtup area from 1973 to 2023. In Table 5, it can be seen that there is a conversion of other land classes into bare open land, but overall, there is a reduction of 14.827% in the bare open land, while there is a small increase (+0.233%) in the water area. This reduction in the flood plain area further diminishes the land's capacity to absorb and store water, intensifying flood risks and migration from rural to urban regions due to a rise in population and urbanisation. Urbanisation is the primary source of changes in hydrologic and hydraulic processes, loss of current drainage capacity, and floods in metropolitan areas. It raises the overall runoff volume and peak discharge during storm runoff occurrences (Zope *et al.*, 2016; Dutta *et al*, 2020). Urbanisation in these areas disrupts the natural flow paths, leading to increased surface runoff, reduced groundwater infiltration, and a higher risk of urban flooding. The absence of natural drainage exacerbates waterlogging during heavy rains, as seen in many urban centres worldwide. Given that human activity is typically the cause of

environmental change, population expansion plays a significant role in determining the LULC pattern (Dewan and Yamaguchi, 2009; Bhuivan *et al.*, 2014; Dang *et al.*, 2018; Akalu *et al.*, 2019; Njiru, 2019; Inalpulat and Genc, 2021; Bisht *et al.*, 2023; Raj and Deswal, 2025).

Additionally, riverbeds often retain a significant ecological function, providing habitats for flora and fauna, which are destroyed when replaced by concrete infrastructure. Expanding urbanisation in such zones can also pose risks to construction due to unstable soil conditions, leading to structural vulnerabilities. Moreover, encroachment on former river paths undermines the natural water cycle and reduces water availability for agriculture and nearby communities, thus intensifying water scarcity.

## CONCLUSIONS

This study shows the evolution of the Land Use Land Cover in the last five decades of the study area, covering a total of 3145.79 sq. km. LULC classification of the study area provides the following conclusions:

- Amongst all the land cover classes, the change in water area is very moderate, while other classes have shown significant change.
- A large part of the agricultural and floodplain area is covered by builtup areas, leading to flooding in the nearby areas.
- Also, bare open land area has shown a significant reduction, which ultimately leads to a decrease in floodplain area.
- The overall accuracy achieved in the study is 94.30% for the 1973 dataset image and 99.50% for the 2023 dataset image, which is satisfactory. Both the accuracy assessment indicates the Kappa coefficient nearer to one.

The findings highlight the need for a comprehensive understanding of the drivers of land use change and the development of sustainable land management strategies to ensure the long-term health and resilience of the ecosystem. Future research should continue to monitor and assess land use and land cover change, investigate the drivers and impacts of these changes, and explore innovative solutions for sustainable land management.

### Acknowledgement

The author acknowledges the guidance and supervision of Prof. Mahesh Pal and Prof. Surinder Deswal, Civil Engineering Department, National Institute of Technology Kurukshetra, India, during this study with all humility.

### Grant Support Details

The present research did not receive any financial support.

### Conflict of Interest

The author declares that there is not any conflict of interest regarding the publication of this manuscript. In addition, the ethical issues, including plagiarism, informed consent, misconduct, data fabrication and/ or falsification, double publication and/or submission, and redundancy, have been completely observed by the author.

## REFERENCES

1) WHO (2025) *Urban health*. World Health Organization. Available at: https://www.who.int/health-topics/urban-health#tab=tab (Accessed: 19 January 2025).
2) Chen, R., Ye, C., Cai, Y., Xing, X. and Chen, Q. (2014) 'The impact of rural out-migration on land use transition in China: past, present and trend', *Land Use Policy*, 40, pp. 101–110. https://doi.org/10.1016/j.landusepol.2013.10.003
3) Nugroho, H.Y.S.H., van der Veen, A., Skidmore, A.K. and Hussin, Y.A. (2018) 'Expansion of traditional land-use and deforestation: a case study of an adat forest in the Kandilo Subwatershed, East Kalimantan, Indonesia', *Journal of Forestry Research*, 29(2), pp. 495–513. https://doi.org/10.1007/s11676-017-0449-9
4) Nabegu, A.B. (2014) 'Impact of urbanization on channel morphology: some comments', *J. Environ. Sci. Toxicol. Food Technol.*, 8(4), pp. 40–45 (2014). DOI: 10.9790/2402-08424045
5) Ibitoye, M.O., Komolafe, A.A., Adegboyega, S.A., Adebola, A.O. and Oladeji, O.D. (2020) 'Analysis of vulnerable urban properties within river Ala floodplain in Akure, Southwestern Nigeria', *Spat. Inf. Res.*, 28(4), pp. 431–44. https://doi.org/10.1007/s41324-019-00298-6
6) Chin, A. (2006) 'Urban transformation of river landscapes in a global context', *Geomorphology*, 79(3–4), pp. 460–487. https://doi.org/10.1016/j.geomorph.2006.06.033
7) Lui, G.V. and Coomes, D.A. (2015) 'A Comparison of novel optical remote sensing-based technologies for forest- cover/change monitoring', *Remote Sens.*, 7, pp. 2781–2807. https://doi.org/10.3390/rs70302781
8) Miller, J..D. and Hess, T. (2017) 'Urbanization impacts on storm runoff along a rural-urban gradient', *Journal of Hydrology*, 552, pp. 474-489. https://doi.org/10.1016/j.jhydrol.2017.06.025
9) Sarker, S. (2022) 'Essence of MIKE 21C (FDM Numerical Scheme): application on the River morphology of Bangladesh', *Open J. Model. Simul.*, 10, pp. 88–117. DOI: 10.4236/ojmsi.2022.102006
10) Yousefi, S., Vfakhah, M., Mirzaee, S. and Tavangar, S. (2013) 'Some changes of morphological parameters of Karoon River using remote sensing (1989-2005)', *Iran Remot. Sens. GIS*, 5, pp. 85–96. https://www.researchgate.net/publication/257264799
11) Zheng, S., Han, S., Tan, G., Xia, J., Wu, B., Wang, K. and Edmonds, D.A. (2018) 'Morphological adjustment of the Qingshuigou Channel on the Yellow River delta and factors controlling its avulsion', *Catena*, 166, pp. 44–55. https://doi.org/10.1016/j.catena.2018.03.009
12) Nones, M. (2021) 'Remote sensing and GIS techniques to monitor morphological changes along the middle-lower Vistula River, Poland', *Int. J. River Basin Manag.*, 19, 345–357. https://doi.org/10.1080/15715124.2020.1742137
13) Kausarian, H., Redyafry, L., Sumantyo, J.T.S., Suryadi, A. and Lubis, M.Z. (2023) 'Structural analysis of the central Sumatra Basin using geological mapping and landsat 8 oli/tirsC2 L1 data', *EVERGREEN Joint Journal of Novel Carbon Resource Sciences & Green Asia Strategy*, 10(02), pp. 792-804. DOI: 10.5109/6792830
14) Moldakhanova, N., Alimkulov, S. and Smagulov, Z. 'Analysis of changes in the ecological space of the Ili river delta (due to reduced flow of the Ili River)', *EVERGREEN Joint Journal of Novel Carbon Resource Sciences & Green Asia Strategy*, 10(01), pp. 29-35. DOI: 10.5109/6781031
15) Zope, P.E., Eldho, T.I. and Jothiprakash, V. (2016) 'Impacts of land use–land cover change and urbanization on flooding: a case study of Oshiwara River Basin in Mumbai, India', *Catena*, 145, pp. 142-154. https://doi.org/10.1016/j.catena.2016.06.009
16) Xu, Y., Xu, Y., Wang, Q., Wu, L., Yang, J. and Shi, H. (2018) 'Relationship between urbanization and river network change in Taihu basin, China', *Adv. Water Sci.*, 29(4), pp. 473–481. http://skxjz.nhri.cn/en/article/doi/10.14042/j.cnki.32.1309.2018.04.003
17) Han, L., Xu, Y., Deng, X. and Li, Z. (2020) 'Stream loss in an urbanized and agricultural watershed in China', *J. Environ. Manag.*, 253, 109687. https://doi.org/10.1016/j.jenvman.2019.109687
18) Yussupov, A. and Suleimenova, R.Z. (2023) 'Use of remote sensing data for environmental monitoring of desertification', *EVERGREEN Joint Journal of Novel Carbon Resource Sciences & Green Asia Strategy*, 10(01), pp. 300-3007. https://www.tj.kyushu-u.ac.jp/evergreen/contents/EG2023-10_1_content/pdf/p300-307.pdf
19) Yermekbayev, B.K., Dzhangarasheva, N.V. and Rakhimzhanova, G.M. 'Overview of grazing as a land use system in Kazakhstan', *EVERGREEN Joint Journal of Novel Carbon Resource Sciences & Green Asia Strategy*, 10(02), pp. 658-666. DOI: 10.5109/6792812

20) Aduah, M., Jewitt, G. and Toucher, M. (2018) 'Assessing impacts of land use changes on the hydrology of a lowland rainforest catchment in Ghana, West Africa', *Water*, 10(1), pp. 9. https://www.mdpi.com/2073-4441/10/1/9#
21) Inalpulat, M. and Genc, L. (2021) 'Quantification of LULC changes and urbanization effects on agriculture using historical landsat data in north-west Anatolia, Turkey', *Polish Journal of Environmental Studies*, 30(5), pp. 3999-4007. https://doi.org/10.15244/pjoes/130953
22) Pranoto, B., Adilla, I., Soekarno, H., Supriatna, N.K., Adrian, Efiyanti, L., Indrawan, D.A., Hesty, N.W. and Fithri, S.R. (2023) 'Using satellite data of palm oil area for potential utilization in calculating palm oil trunk waste as cofiring fuel biomass', *EVERGREEN Joint Journal of Novel Carbon Resource Sciences & Green Asia Strategy*, 10(03), pp. 1784-1791. https://doi.org/10.5109/7151728
23) Wentz, E.A., Nelson, D., Rahman, A., Stefanov, W.L. and Roy, S.S. (2008) 'Expert system classification of urban land use/cover for Delhi, India', *International Journal of Remote Sensing*, 29(15), pp. 4405–4427. https://doi.org/10.1080/01431160801905497
24) Napieralski, J.A. and Carvalhaes, T. (2016) 'Urban stream deserts: mapping a legacy of urbanization in the United States', *Appl. Geogr*., 67, pp. 129–139. https://doi.org/10.1016/j.apgeog.2015.12.008
25) Msofe, N.K., Sheng, L. and Lyimo, J. (2019) 'Land use change trends and their driving forces in the Kilombero Valley floodplain, southeastern Tanzania', *Sustainability*, 11(2), pp. 505. https://doi.org/10.3390/su11020505
26) Shahfahad, M., Mourya, B., Kumari, M., Tayyab, A., Asif, P. and Rahman, R. (2021) 'Indices based assessment of built-up density and urban expansion of fast growing Surat city using multi-temporal Landsat data sets', *GeoJournal*, 86, pp. 1607-1623. https://doi.org/10.1007/s10708-020-10148-w
27) Gorelick, N., Hancher, M., Dixon, M., Ilyushchenko, S., Thau, D. and Moore, R. (2017) 'Google Earth Engine: planetary-scale geospatial analysis for everyone', *Remote Sens. Environ.*, 202, pp. 18–27. https://doi.org/10.1016/j.rse.2017.06.031
28) Phan, T.N., Kuch, V. and Lehnert, L.W. (2022) 'Land cover classification using Google Earth Engine and Random Forest Classifier—the role of image composition', *Remote Sens.*, 12(15), 2411. https://doi.org/10.3390/rs12152411
29) Dutta, D., Rahman, A., Paul, S.K. and Kundu, A. (2020) 'Estimating urban growth in peri-urban areas and its interrelationships with built-up density using earth observation datasets', *The Annals of Regional Science*, 65, pp. 67-82. https://doi.org/10.1007/s00168-020-00974-8
30) Dewan, A.M. and Yamaguchi, Y. (2009) 'Land use and land cover change in Greater Dhaka, Bangladesh: using remote sensing to promote sustainable urbanization', *Appl. Geogr.*, 29, pp. 390–401. https://doi.org/10.1016/j.apgeog.2008.12.005
31) Akalu, F., Rade, J.M., Sintayehu, E.G. and Kiptala, J. (2019) 'Evaluation of land use and land cover change (1986-2019) using remote sensing and GIS in Dabus Sub-catchment, Southwestern Ethiopia', *Journal of Sustainable Research in Engineering*, 5(2), pp. 91-100. https://doi.org/10.1007/s42452-021-04498-4
32) Njiru, E.B.K. (2019) 'Urban expansion and loss of agricultural land: a GIS based study of Kiambu County', *International Journal of Science and Research*, 8(9), pp. 915. https://www.ijsr.net/archive/v8i10/ART20201852.pdf
33) Bisht, P., Deswal, S. and Pal, M. (2023) 'Land surface temperature extraction using landsat data over Dehradun, India: assessment of various retrieval algorithms and emissivity models', *Suranaree J. Sci. Technol.*, 30(6), pp. 010282(1-11). DOI : 10.55766/sujst-2023-06-e02912
34) Bhuivan, M.A.H., Kumamoto, T. and Suzuki, S. (2014) 'Application of remote sensing and GIS for evaluation of the recent morphological characteristics of the lower Brahmaputra-Jamuna River, Bangladesh', *Earth Sci. Informatics*, 8, pp. 551–568. https://okayama.elsevierpure.com/en/publications/application-of-remote-sensing-and-gis-for-evaluation-of-the-recen
35) Dang, X., Xu, Y., Han, L., Song, S., Xu, G. and Xiang, J. (2018) 'Spatial-temporal changes in the longitudinal functional connectivity of river systems in the Taihu Plain, China', *J. Hydrol.*, 566, pp. 846–859. https://doi.org/10.1016/j.jhydrol.2018.09.060
36) Raj, S. and Deswal, S. (2025) 'Land-use land-cover classification and its change detection using multi-temporal landsat data', *International Journal of Technology, Health and Sustainability*, 1(1), pp. 13-24. https://ijths.com/wp-content/uploads/2025/09/ijths-010113.pdf